

## Establishing the Threshold Condition for Soil Movement in Wind-Eroding Fields

**John E. Stout & Ted M. Zobeck**

Wind Erosion Research Unit  
USDA-Agricultural Research Service  
Lubbock, TX 79401

### Abstract

*One of the most basic features of a wind eroding surface is its threshold velocity – the wind velocity at which soil movement is initiated and dust is generated. Many theoretical equations and numerical models of the wind erosion process include threshold as an important basic parameter. SENSIT, an instrument that uses a piezoelectric crystal to count particle impacts, provides a means of indirectly measuring threshold in the field. If we simultaneously observe the number of particle impacts and the wind speed then, in principle, it is possible to detect the lowest wind velocity where particle impacts are first recorded. Unfortunately, under typical field conditions with gusty turbulent winds and mixed sediment soils the correlation between wind velocity and soil movement is weakened due to many factors. As a result it is hard to accurately pinpoint a single representative value of threshold by direct observation. We have developed a new method, called the “time fraction equivalence method”, which eliminates this problem. This method is based upon the principle that the fraction of time that erosion occurs should be equivalent to the fraction of time that winds exceed threshold. We simply have to determine the value of threshold that yields this equivalence. Example threshold calculations using the “time fraction equivalence method” are presented from data taken during a study in an agricultural field in New Deal, Texas.*

### Introduction

It is generally accepted that the generation of dust from sandy soils is intimately linked to the action of saltating grains (Gillette *et al.*, 1974; Shao & Raupach, 1993). Sand grains bouncing across the surface pulverize the soil releasing clouds of fine particles that then become suspended in turbulent winds. Unlike sand grains, which often deposit in dunes at the edge of the eroding field, dust is sometimes transported vast distances across the continent, representing a true soil loss and a major source of air pollution (Gillette, 1977).

Ideally one would like to be able to predict periods of saltation-induced dust generation from a measured wind velocity record. To do so requires knowledge of the critical threshold condition for soil movement.

In the past, wind tunnel tests have been used to establish the threshold condition for soil movement (Bagnold, 1941; Kawamura, 1951; Zingg, 1953; Nickling, 1988). Typically, a soil surface is transplanted from the field into the test

section of a wind tunnel, the wind speed is adjusted, and the critical wind speed at which soil movement is initiated is noted. The wind tunnel provides a controlled environment that allows a careful and systematic study of the threshold condition. The determination of threshold under natural field conditions is more difficult.

In the naturally turbulent atmosphere, rapid and chaotic wind fluctuations preclude controlled experiments. Yet we need to venture to the field to study the threshold condition if we wish to obtain a true picture of the wind erosion process under realistic conditions. For example, it is difficult to properly simulate the full spectrum of fluid motions within a laboratory wind tunnel (Snyder, 1981). The turbulence characteristics within the atmospheric boundary layer are established as the wind blows across vast stretches of the earth's surface, and it is hard to reproduce these same characteristics within the limited fetch of a wind tunnel test section. Furthermore, the transplanted soil surface in most wind tunnel experiments does not properly represent the actual soil conditions within the field. Certainly, these problems could be overcome with a great deal of cleverness and an equally large budget, but perhaps it is of more practical value to improve the method of direct determination in the field.

Here we report results from a field experiment in which we used the intermittency of the wind erosion process and recent advances in instrumentation to establish the threshold wind speed under natural field conditions. This was accomplished by simultaneously monitoring soil movement and wind velocity at a single location within the field at a frequency of 1 Hz.

### Study Area

The experimental site was a privately owned agricultural field near the small town of New Deal, Texas just north of Lubbock. The field lies within the southernmost part of the Great Plains called by various names including the Southern High Plains or the Llano Estacado (Staked Plains). This region is characterized by a thin mantle of sediment that overlies a calcrete caprock. In its natural state, it is a broad short-grass prairie with few trees or other large plants (Brown, 1979). The region is mostly flat except for many shallow saucer-like depressions called playa lakes. The climate is semiarid, receiving annual precipitation of around 450 mm per year, most of which falls during the summer months (Bomar, 1983). This area is known as one of the flattest, most windswept, and featureless regions in North America.

Today, the Llano Estacado region is under intensive agriculture. Cotton, wheat, sorghum, and other grains are grown on vast tracts of land. During a successful growing season, vegetative cover is often sufficient to protect the soil

surface from the nearly incessant winds but during occasional droughts, plant establishment can fail leaving the soil bare and vulnerable. Plants such as cotton leave little residue after harvest leaving the soil unprotected. In the late winter and spring, exposed soils, high winds, and low soil moisture combine to produce massive and frequent dust storms.

Kerry Weinheimer and Randy Underwood of the Lubbock NRCS mapped the topography of the field as shown in Fig. 1. The field gradually sloped downward toward a playa lake that was completely dry at the time of the experiment. Near the experimental site, denoted by a star, the slope gradient was around 3%. The mean wind, denoted by an arrow, blew upslope at an angle of about 30° to the contours.

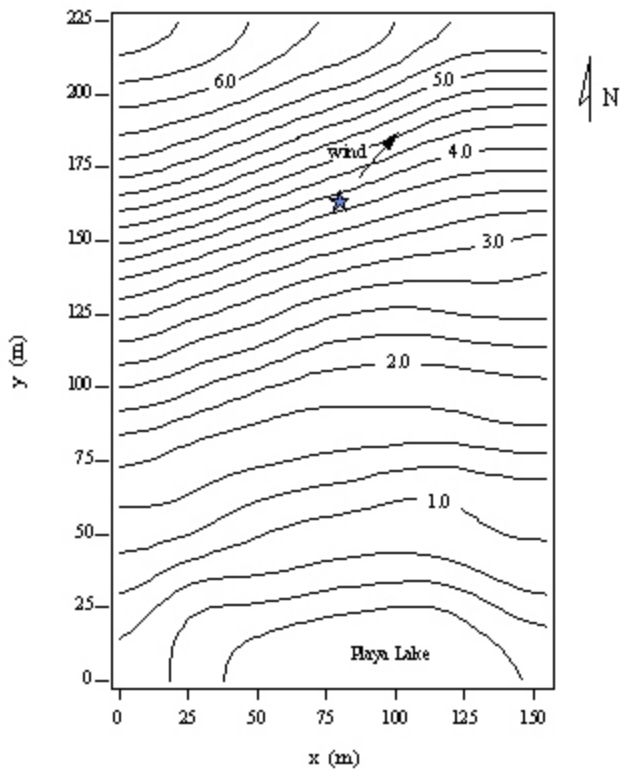


**Figure 1.** Topography of the study area. A star denotes the point of measurement (33° 42' 11" N, 101° 49' 12" W).

The soil type was a borderline sandy clay loam with 21% clay, 11% silt, and 68% sand. Organic matter content was a mere 1.7%. During the previous summer the field was planted to wheat but due to drought conditions, the wheat crop failed leaving a bare surface with little residual plant material. The surface had little roughness except for some heavily weathered chisel tracks that ran north/south and a few clumps of weeds sprouting here and there. Using the chain method developed by Saleh (1994), the physical surface roughness was found to be 4% and from measured wind profiles, the aerodynamic roughness  $z_0$  was found to be 0.0005 m.

## Experimental System

The experimental system consisted of a portable 2-m meteorological tower, a SENSIT piezoelectric saltation monitor, and a data logger for recording their output. Data was recorded at a frequency of 1 Hz.

Wind velocities were measured using lightweight, fast-responding cup anemometers mounted at heights corresponding to 0.15, 0.38, 0.77, and 2.0 m. The responsiveness of such anemometers is typically given in terms of a distance constant which is the length of travel of an airstream required for the instrument to respond to 63% of a step change in velocity. In this case, the distance constant is 2.3 m. The time response of the anemometer can be obtained by dividing the distance constant by the wind speed to obtain the time constant. A wind speed of 10 m/s yields a time constant of 0.23 s; higher wind speeds improve the time response of the anemometer. The mean 2-m wind speed during this storm was 10.55 m/s, so we could safely sample the wind velocity at a frequency of 1 Hz.

Wind erosion was monitored by counting the number of particles that impact a piezoelectric sensing element each second. The SENSIT instrument, shown in Fig. 2, outputs a pulse signal proportional to the number of particle impacts (Gillette & Stockton, 1986; Stockton & Gillette, 1990).

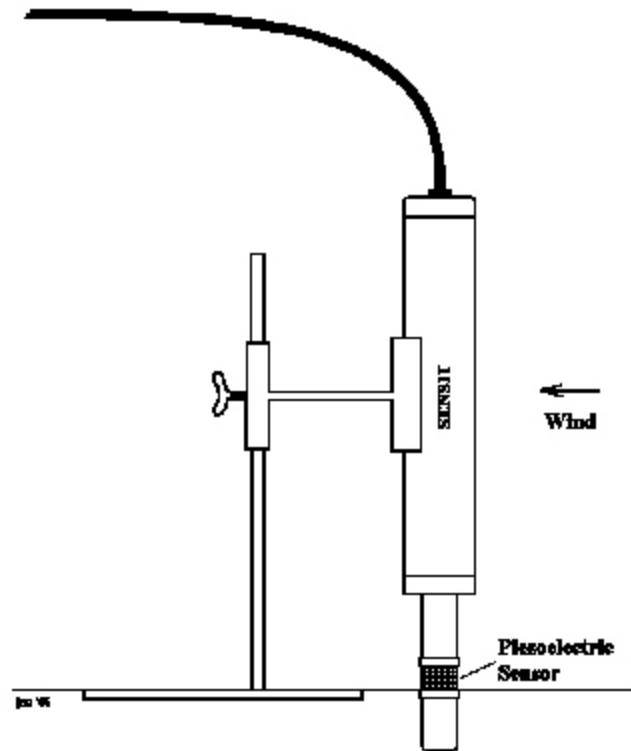


**Figure 2.** Drawing of SENSIT, a saltation sensor.

As shown in Fig. 2, SENSIT was mounted so that the lower edge of the sensing crystal was flush with the eroding surface. The cylindrical sensing element extended from the

surface to a height of 13 mm. The diameter of the sensing element was 25 mm forming a total impact area of 325 mm<sup>2</sup>. Since particles that glance off the edges of the crystal have a lower probability of being detected, the effective sampling area is actually less than the frontal area of the crystal. The number of particle impacts divided by the one-second sampling interval yields a value of particle impacts per second.

As explained in Stockton & Gillette (1990), the sensitivity of the piezoelectric crystal was purposely adjusted so that it primarily responds to the impact of saltating grains. This adjustment excludes wind vibration or electrostatic noise that could contaminate the signal. The instrument also does not respond to the movement of fine dust grains since fine particles normally follow the airflow around the sensing element and thereby fail to impact. Even if a fine dust speck were to impact the piezoelectric crystal, the momentum transfer would be too low to trigger a pulse.

We recently completed a series of laboratory tests of SENSIT's sensitivity using impacting glass beads. These tests reveal that the piezoelectric crystal does not respond to particles with momentum less than  $5 \times 10^{-8}$  N s. Particle momentum is the product of particle mass and velocity, so a small particle moving quickly can have the same momentum as a large particle moving slowly. The minimum velocity of a given diameter sand grain (particle density of 2650 kg/m<sup>3</sup>) that yields a particle momentum of  $5 \times 10^{-8}$  N s is calculated in Table 1. The calculations suggest that it is unlikely that SENSIT responds to particles with diameter less than 100  $\mu$ m since it is nearly impossible for such grains to attain a speed of 36 m/s during a typical wind erosion event. However, the erosion sensor will most likely respond to particles larger than 200  $\mu$ m since the required particle speed is generally less than typical wind speeds associated with dust storms. Because SENSIT only responds to impacts of larger grains, it acts primarily as a saltation sensor.

**Table 1.** Required velocity of particle with diameter D to achieve minimum detectable momentum value of  $5 \times 10^{-8}$  N s.

D ( $\mu$ m)	Mass (kg)	Velocity. (m s <sup>-1</sup> )
100	1.39E-09	36.04
150	4.68E-09	10.68
200	1.11E-08	4.50
300	3.75E-08	1.33
400	8.88E-08	0.56
500	1.73E-07	0.29
600	3.00E-07	0.17
700	4.76E-07	0.11
800	7.10E-07	0.07
900	1.01E-06	0.05
1000	1.39E-06	0.04

Since dust can be generated far upwind and transported vast distances, the presence of dust is not a reliable indicator of erosion activity at a single point of measurement. The presence of saltation activity, however, clearly indicates that erosion is occurring at the point of measurement. Thus, the fact that SENSIT fails to respond to the movement of fine particles is a positive feature since the selective signal from SENSIT is a clear indication of the level of saltation activity at a given point within the field.

Initially, there was some concern whether this selective feature allows one to detect the earliest signs of soil movement. We attempted to visually confirm that SENSIT is providing a true picture of erosion activity by simultaneously observing SENSIT output and saltation activity near the instrument during a dust storm. We concluded that the detectable momentum limit of the sensing element ( $5 \times 10^{-8}$  N s) is sufficiently small to allow detection of any significant saltation activity capable of generating dust.

## Results and Discussion

The storm occurred during the afternoon of April 14, 1995. We were able to collect data for six separate periods from 1451 to 1615 local time. Wind profile data and SENSIT values were recorded simultaneously at a frequency of 1 Hz. Due to memory limitations, the data logger could not store data for periods longer than 9 minutes 26 seconds. When the memory became saturated, data acquisition had to be halted as the acquired data set was transferred to a portable computer. As a result the data consist of individual packets of high frequency data taken at different times during the storm.

A plot of wind direction  $\theta(t)$ , 2-m wind speed  $u(t)$ , and wind erosion activity  $p(t)$  as measured during each sampling period is shown in Figs. 3 to 5. Mean values are denoted by horizontal dashed lines. Overall, the wind direction varied from 186° to 282° with a mean of 230° and a standard deviation of 14°. The wind speed varied from a minimum of 5.55 m/s to a maximum of 17.73 m/s with a mean of 10.55 m/s and a standard deviation of 1.80 m/s.

Qualitatively there appears to be a fairly good correlation between wind speed and saltation activity; strong gusts are generally associated with strong erosion activity. However, a careful examination reveals a less than perfect match. There are many possible explanations for this imperfect correlation. One possibility is that inertial effects produce a natural time delay between the moment the wind exceeds threshold and the resulting movement of soil particles. The same effect can occur when the wind drops below threshold and particles are still airborne. Thus, soil movement may lag wind forcing.

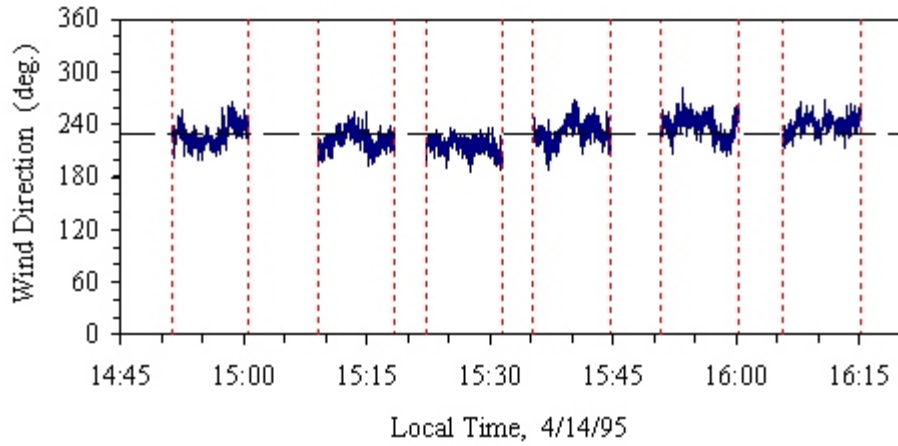


**Figure 3.** Wind direction.

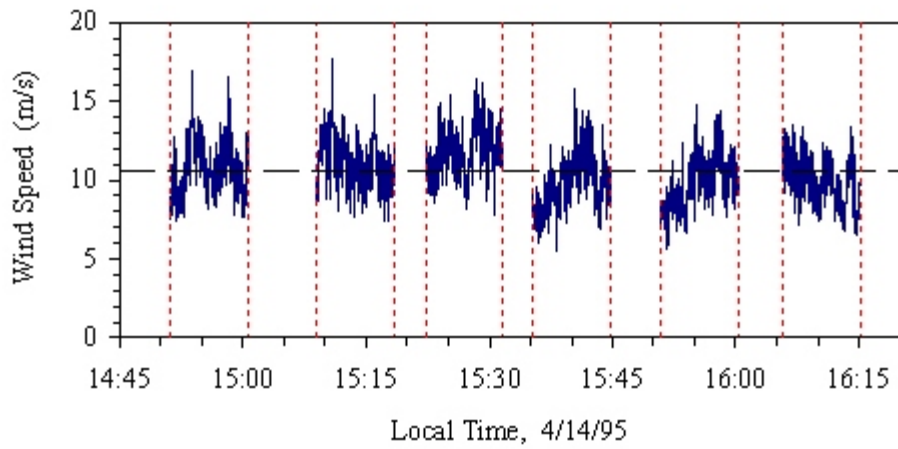


**Figure 4.** Wind speed.

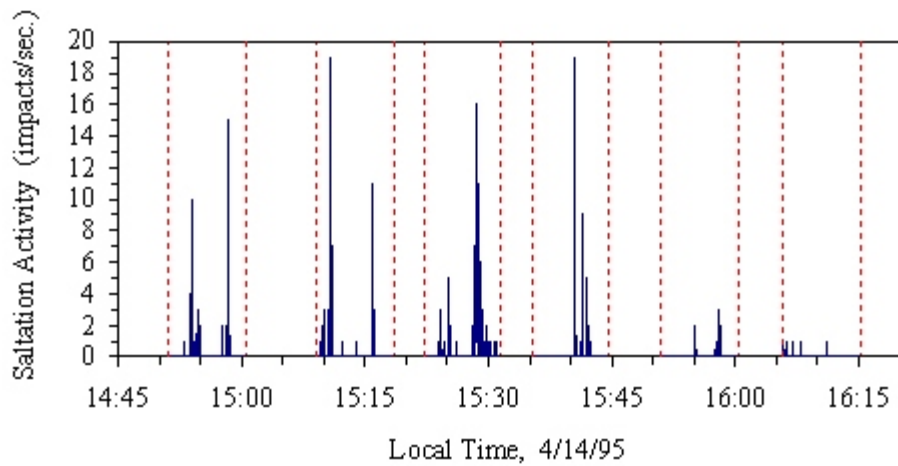


**Figure 5.** Saltation activity expressed in units of particle impacts per second.

It is possible to estimate this natural time lag from the wind and saltation activity records by calculating the cross correlation between wind velocity  $u(t)$  and saltation activity  $p(t)$ . The cross correlation coefficient may be expressed as:

$$r_{up}(\tau) = \frac{\overline{(u(t) - \bar{u})(p(t + \tau) - \bar{p})}}{\sigma_u \sigma_p} \quad (1)$$

where  $\tau$  denotes time lag, the overbar denotes a mean quantity, and  $\sigma_u$  and  $\sigma_p$  are the standard deviation of wind velocity and saltation activity, respectively. The calculated cross correlation between wind speed and saltation activity yields Fig. 6. Note that the peak occurs at a lag time of approximately one second indicating that saltation activity typically lags wind speed by about one second. Wind tunnel experiments reported by Butterfield (1991) indicate that saltation systems respond to flow changes within one to two seconds. A numerical simulation reported by Anderson & Haff (1988) also suggest that the response time of the saltation system is approximately one to two seconds.

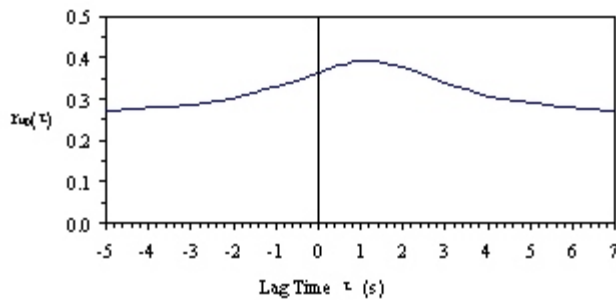


Figure 6 Cross correlation between wind velocity and saltation activity.

### Scatter Plot

Another useful way of looking at the relationship between wind forcing and saltation activity is to simply plot saltation activity as a direct function of wind velocity, thereby, removing time as a variable (Fryrear *et al.*, 1991; Thorne *et al.*, 1989; Gillette *et al.*, 1995). The resulting scatter plot, shown in Fig. 7, reveals that in most cases large values of erosion activity are associated with large wind velocities. However, the large amount of scatter reveals an imperfect correlation between these two variables.

Plotting the 1-second lagged saltation activity  $p(t+1)$  as function of  $u(t)$  slightly reduces the scatter as shown in Fig. 8 but a considerable amount of scatter still remains.

We conclude that the scatter plot provides a reasonable estimate of the threshold range but it is of limited value in establishing a single representative value for the critical threshold condition.

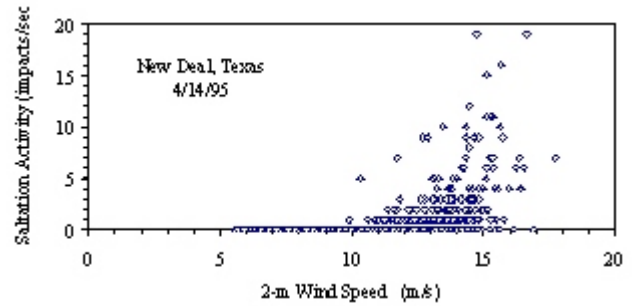


Figure 7. Scatter plot of saltation activity as a function of wind speed.

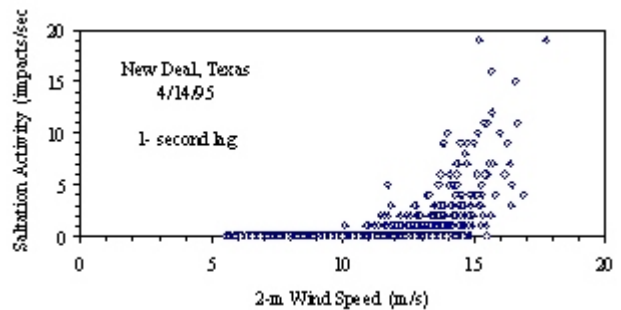


Figure 8. Scatter plot of 1-second lagged saltation activity as a function of wind speed.

### Time Fraction Equivalence

A single representative value of threshold can be obtained by comparing the wind velocity and erosion activity records. The guiding principle of this method is that the fraction of time that erosion occurs should be equivalent to the fraction of time that the wind exceeds threshold. We simply have to determine by iteration the value of threshold that yields this equivalence. Here, we divided each 9-minute sampling interval into 3-minute subintervals which contain 180 lines of data apiece. Within each subinterval we calculated the fraction of time particle impacts were detected. The method for calculating this time fraction is discussed below.

The raw data consists of three columns: time, 2-m wind velocity  $u(t)$ , and SENSIT particle impacts per second  $p(t)$ . First we directly calculate the intermittency factor for particle impacts  $b_p(t)$  as

$$\begin{aligned} b_p(t) &= 0 & \text{if } p(t) &= 0, \\ b_p(t) &= 1 & \text{if } p(t) > 0. \end{aligned} \quad (2)$$

Next we choose an initial guess for the critical threshold value, then calculate the intermittency factor for the wind velocity  $b_u(t)$  as

$$\begin{aligned}
 b_p(t) &= 0 \quad \text{if } u(t) < u_t, \\
 b_p(t) &= 1 \quad \text{if } u(t) \geq u_t.
 \end{aligned}
 \tag{3}$$

Note that for both intermittency factors, a value is obtained for each second of each sampling period. Thus, the original time series for both wind speed and wind erosion are transformed into a digital series of 0's and 1's.

Intermittency functions  $\gamma_p$  and  $\gamma_u$  are then calculated by summing the amount of time that saltation activity was recorded then dividing by the 3-minute sampling interval. Since we sampled wind speed and saltation activity at a regular interval of once per second, the intermittency function for each 3-minute period may be obtained simply by taking the average of the 1-sec intermittency factors as follows:

$$\begin{aligned}
 \gamma_p &= \frac{1}{N} \sum_{i=1}^N b_{p_i}, \\
 \gamma_u &= \frac{1}{N} \sum_{i=1}^N b_{u_i}.
 \end{aligned}
 \tag{4}$$

where in this case  $N = 180$ .

As long as the averaging time is much greater than the natural lag time, soil movement should account for the same fraction of time that winds exceed threshold. In other words,  $\gamma_u$  should equal  $\gamma_p$  if we have chosen the correct threshold  $u_t$ . If  $\gamma_u > \gamma_p$  then the initial guess for  $u_t$  is increased so that  $\gamma_u$  is reduced. If  $\gamma_u < \gamma_p$  then  $u_t$  is decreased so that  $\gamma_u$  is increased. This process is repeated over many iterations until  $\gamma_u = \gamma_p$ . The final value of  $u_t$  that satisfies this equality is considered the critical threshold. This provides a quantitative means of calculating threshold.

Using this method, a threshold value was calculated for each 3-minute period and the results are presented in Table 2. The first column contains the midpoint time of each 3-minute period. The next three columns contain the 3-minute average wind direction, 2-m wind speed, and the standard deviation of the wind velocity. The fifth column contains the intermittency function which represents the fraction of time that saltation activity occurred during each 3-minute period. The last column contains the value of threshold calculated by the time fraction equivalence method. Note that at least one particle impact must be detected ( $\gamma_p$  must be greater than zero) before threshold can be established.

It is important to note here that high frequency sampling of wind erosion activity and wind velocity is necessary to obtain an accurate description of their temporal variation. Butterfield (1993) recommends sampling frequencies of at least 1 Hz if realistic and useful information is to be derived from such experiments. Sampling at 1 Hz appears to be sufficient to properly resolve the intermittency factor.

**Table 2.** Calculated intermittency and threshold.

Time	Mean Wind Dir. (deg.)	Mean Wind Speed (m/s)	Std. Dev. u (m/s)	Interm. Funct. p	Critical Thresh. $u_t$ (m/s)
14:52:45	226	10.41	1.93	0.095	13.34
14:55:54	221	10.91	1.28	0.026	13.64
14:59:03	239	10.94	1.68	0.095	13.08
15:10:36	219	11.91	1.61	0.138	13.61
15:13:45	230	10.66	1.42	0.021	13.5
15:16:53	219	10.73	1.46	0.059	13.4
15:23:46	218	11.49	1.5	0.070	13.95
15:26:53	217	11.7	1.59	0.107	13.8
15:30:00	213	12.37	1.66	0.269	13.3
15:36:48	224	8.47	1.23	0	*
15:39:57	240	10.56	1.58	0.111	12.68
15:43:06	234	10.43	1.63	0.074	13.1
15:52:26	243	8.35	1.11	0	*
15:55:35	244	10.14	1.24	0.016	12.8
15:58:44	229	11.01	1.43	0.080	13.11
16:07:14	238	10.81	1.31	0.021	13.1
16:10:23	242	9.83	1.19	0.005	12.3

The results indicate that this wind erosion event was very intermittent. The largest value of  $\gamma_p$  was 0.269, which indicates that saltation activity accounted for only 27% of this 3-minute period. Typically, saltation activity accounted for less than 10% of the total time. As the wind abated toward the end of the storm the saltation activity reduced to below 1%.

The values of threshold are plotted as a function of time in Fig. 9. There is a slight downward trend in calculated threshold values with time. Fitting a line to the data we find that the slope is -0.64 m/s each hour. This may indicate that as the storm progressed, the breakdown of surface crusts and clods by the bombardment of saltating grains was producing a smoother surface with more loose erodible material; a surface that was becoming slightly more erodible with time (Gillette *et al.*, 1995).

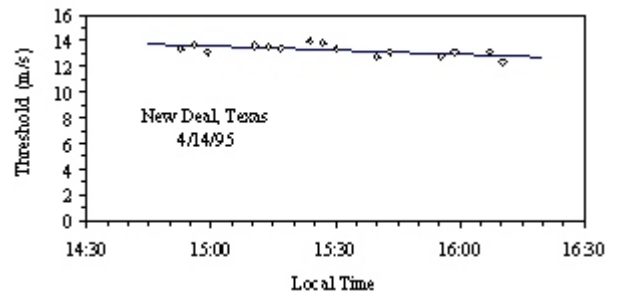


**Figure 9.** Calculated values of threshold wind speed (taken at a height of 2 m) plotted as a function of time.

If we remove the downward trend we find that the variation of calculated threshold values is typically less than 2%. Thus, we conclude that the time fraction equivalence method is a fairly robust and reliable method for objectively establishing the critical threshold of soil movement in the field.

## Conclusions

During marginal wind erosion events, when the mean wind speed is near threshold, turbulent wind fluctuations may intermittently exceed threshold resulting in bursts of saltation activity interspaced with periods of inactivity. During this field experiment we found that saltation activity often accounted for less than 10 % of each measurement period and the maximum time fraction was found to be only 27%. Thus, the majority of soil movement and dust generation was found to occur for a minority of the total time.

Intermittent storms provide an opportunity to establish the critical threshold condition of the soil surface. By simultaneously measuring saltation activity and a reference wind speed at a frequency of 1 Hz it was possible to determine the threshold wind speed which satisfied the condition that the fraction of time that the wind exceeds threshold is equivalent to the fraction of time that saltation activity occurs. The principle of time fraction equivalence provides an objective means for establishing the threshold condition for soil movement under natural field conditions.

We have shown that by using the time fraction equivalence method, threshold can be established with enough precision to identify general trends in the data. Using this method, the threshold wind speed (taken at a height of 2 m) was found to be around 13.5 m/s at the start of the experiment and decreased at a rate of about -0.64 m/s per hour. We suggest that such a change of threshold indicates that the field was becoming more erodible with time.

**Acknowledgments.** We would like to acknowledge the hard work of H. Dean Holder and Bret Lamblin for constructing the equipment used in this experiment and for venturing into the raging dust storm to help obtain the data reported here. I would also like to thank Jeff A. Lee and Tom E. Gill for their careful reviews of this manuscript.

## References

- Anderson, R. S. & P. K. Haff. 1988. Simulation of eolian saltation. *Science* **241**:820-823.
- Bagnold, R. A. 1941. **The Physics of Blown Sand and Desert Dunes.** Methuen, London, 265pp.
- Bomar, G. W. 1983. **Texas Weather.** University of Texas Press, Austin, 265 pp.
- Brown, L. 1979. **Grasses, an identification guide.** Houghton Mifflin, New York, 240 pp.
- Butterfield, G. R. 1991. Grain transport in steady and unsteady turbulent airflows. *Acta Mechanica Suppl.* **1**:97-122.
- Butterfield, G. R. 1993. Sand transport response to fluctuating wind velocity. **Turbulence: Perspectives on Flow and Sediment Transport.** John Wiley & Sons, pp. 305-335.
- Fryrear, D.W., J.E. Stout, L.J. Hagen, & E.D. Vories. 1991. Wind Erosion: Field Measurements and Analysis. *Trans. ASAE*, **34**(1):155-160.
- Gillette, D.A., Blifford, I. H. & Fryrear, D. W. 1974. The influence of wind velocity on the size distributions of aerosols generated by the wind erosion of soils. *J. Geophys. Res.*, **79**:4068-4075.
- Gillette, D. A. & P. H. Stockton. 1986. Mass, Momentum and Kinetic Energy Fluxes of Saltating Particles. **Aeolian Geomorphology**, ed. by W. G. Nickling, Allen and Unwin, Boston, pp.35-56.
- Gillette, D. A., G. Herbert, P. H. Stockton & P. R. Owen. 1995. Causes of the Fetch Effect in Wind Erosion. *Earth Surface Processes and Landforms.* In Press.
- Kawamura, R. 1951. Study on sand movement by wind. Institute of Science and Technology, Tokyo, Report 5, pp. 95-112.
- Nickling, W. G. 1988. The initiation of particle movement by wind. *Sedimentology* **35**:499-511
- Saleh, A. 1994. Measuring and predicting ridge-orientation effect on soil surface roughness. *Soil Sci. Soc. Am. J.* **58**:1228-1230.
- Shao, Y., M. R. Raupach & P. A. Findlater. 1993. Effect of saltation bombardment on the entrainment of dust by wind. *J. Geophys. Res.*, **98**:12719-12726.
- Snyder, W. H. 1981. Guideline for fluid modeling of atmospheric diffusion. EPA-600/8-81-009.
- Stockton, P. & D.A. Gillette. 1990. Field measurements of the sheltering effect of vegetation on erodible land surfaces. *Land Degradation & Rehabilitation* **2**:77-85.
- Thorne, P. D., Williams, J. J. and Heathershaw, A. D. 1989. In situ measurements of marine gravel threshold and transport. *Sedimentology* **36**:61-74.
- Zingg, A.W. 1953. Wind tunnel studies of the movement of sedimentary material. Proceedings 5th Hydraulic Conference Bulletin, **34**:111-35.